Highly Selective Capture and Transport of Rare Cells in Microfluidic Channels

M.D. Ward and P. Grodzinski

Los Alamos National Laboratory, B-4 MSJ586,
Los Alamos, NM, USA, wardmd@lanl.gov

ABSTRACT

Collection of rare target cells in clinical samples such as disseminated tumor cells in peripheral blood, poses difficult challenges to currently available cell separation methods. A novel, two stage microfluidic system enabling highly efficient and specific concentration of rare target cells has been developed. It uses immunomagnetic separation in fluidic channels to isolate target cells to nanoliter volumes from milliliters of blood. Particle trajectory modeling accurately predicts optimal flow rates for near 100% efficient capture. In the first stage a magnetic gradient is applied to a shallow channel. Experiments using model cells spiked into mouse blood suggest the devices could outperform the current immunocytochemistry gold standard for selectivity of $1 : 10^6$ (rare target cells : white blood cells).

Keywords: immunomagnetic, cancer, microfluidic, cell separation.

1 INTRODUCTION

The past two decades have seen a steadily increasing importance in the application of immunomagnetic separation methods to biological problems in medical, food and pharmaceutical industries, biothreat detection and basic research. Transferring some of these methods to the world of microfluidics promises reduced cost, high throughput and automation for important immunomagnetic assays and offers the possibility of new applications through integration with microfluidic components. Several groups have begun to manipulate magnetically labeled targets in the microfluidic environment for applications as varied as hybridization assays [1] to hematology [2].

Follow up diagnosis of post-treatment cancer patients and screening for cancer of healthy patients are clinical tasks that researchers have long sought to address with disseminated tumor cells from bone marrow and or peripheral blood. While pre –disease screening remains a distant clinical reality, the use of disseminated tumor cells (DTCs) for prediction of prognosis and prescription of adjuvant therapy has been studied by many groups over the last decade. Independent prognostic value has been indicated by many studies for many different types of cancers.

Some studies indicate conflicting results regarding prognostic value however, and more research must be done. It has been suggested that some of the discrepancies may lie in inconsistent processing of patient samples [3] and or method for determination of DTCs. Standardization of procedures will be a necessary step in the evaluation of clinical significance of DTCs, particularly in the area of sample preparation [4]. Automated analysis systems have the potential of providing this standardization if they can be made sensitive, specific and inexpensive enough to compete with current methods. The gold standard right now for sensitivity and specificity is immunocytochemistry.

This is very labor intensive however, as several slides of blood or bone marrow may have to be examined in order to find even a single disseminated cell. The devices tested herein could facilitate a path to automation that would reduce labor costs. They could also provide a platform that enables a combination of integrated analysis that might lead to superior diagnostic information. Such a device might be capable for example, of counting disseminated tumor cells, allowing examination of morphologic and immunological properties and performing molecular analysis such as RT-PCR. The first step in realizing such a device is the assessment of efficiency, specificity and purity of capture in the cell concentration/purification stage of an integrated device. The primary aims of this research were to assess capture efficiency in prototype devices and compare this with the predictions of the models developed for the devices.

2 METHODS

The methods for this research can be readily divided into three basic categories. The first is selection and immunomagnetic labeling of model cells, which includes determination of the cell's magnetic moment. The second is capture device design and fabrication and the third is modeling of the model cells in the devices.

2.1 Model cells and magnetic labeling

In order to more easily asses the performance of the mathematical models, microspheres with fairly consistent magnetic label binding properties were chosen as model cells. The average velocity of a population of microspheres in a known magnetic field and gradient can be correlated to the number of targeted receptors on a cell's surface [5]. This allows for a simple prediction for cell populations of interest with available receptor density data.

Commercial colloidal immunomagnetic labels from Miltenyi Biotec GmbH, (Bergisch Gladbach, Germany) were used for all experiments. While these labels are only approximately 50 nm in diameter and have a much smaller magnetic moment than their particulate class (>1 micron) counterparts, they have several advantages over such labels: 1) Colloids are well mixed in solution without settling 2) Colloids will not interfere with optical imaging or detection 3) Labeling with colloids is faster and more efficient 4) Colloids will not clump together and obstruct micro-channels.

The typical labeling protocol is outlined below. Fifty µl Phyco-erythrin coated microspheres, catalog code 1203 (Bangs Laboratories, IN) were added to 950µl of phosphate buffered saline pH 7.4 without calcium or magnesium with 0.1% pluronic F68 (BASF) and 5mM EDTA. 5 µl anti-PE microbeads were added to the buffer/ bead mix and the solution was vortexed for 10 seconds and placed on a rotating mixer for 2 hours. While this long incubation is not necessary, it insures saturated equilibrium binding. For experiments involving 50% citrated mouse blood, steps were identical except that the blood was substituted for half the buffer volume.

Video of particles flowing in a 95 µm high x 3mm wide channel and exposed to a knowmn magnetic gradient was recorded for determination of magnetic velocity. Video was digitized using Adobe premiere and was saved as a sequence of individual bitmap files with 29.97 frames per actual second of analog video footage. Particle positions were tracked through the sequence of frames using Scion Image analysis software. Particles making their way to the capture surface appear as streaks in each recorded frame. To determine velocities of these particles, the pixel length of the streak was recorded and converted to a length. This length times the frame rate of 30 sec^{-1} gives particle velocity. If it assumed that the particle velocity follows the parabolic laminar flow streamlines at distances far from the wall, then velocities from frame to frame can be compared to the calculated velocity of a streamline for a given height in the channel. In this way it is then possible to track the particle velocity in the direction of the height of the channel. This is the magnetic velocity plus the sedimentation velocity for a non-neutrally buoyant particle. The sedimentation velocity is determined separately with the magnetic field removed and can be subtracted to determine magnetic velocity alone.

By moving the low gradient channel away from the magnet structure using plastic spacers it was possible to measure magnetic velocity for smaller gradients and fields. In this way it was possible to do experiments for lower magnetic velocities using the same population of microspheres. In practice, this would correspond to the cells with fewer targeted receptors in the higher field and gradient.

For the high gradient channel the magnet position was fixed so the model was assessed by changing wire lengths and materials. Nickel wire lengths of 10 and 25 mm and a nickel iron wire length of 25 mm were tested.

2.2 Device design and Fabrication

Channels were formed by laser cutting desired channel shapes in 100µm thick double sided tape (Adhesives Research) and top and bottom acrylic lids with an engraving laser (Universal Laser Systems, Scottsdale, AZ). Structures were simply aligned and pressed together to achieve a bond. For the high gradient channel a nickel or nickel iron wire was laid into the channel before bonding the top piece. Low and high gradient channels were tested separately for assessment of the mathematical models. The integrated system is shown in figure 1.

In the integrated system, magnetically labeled cells are drawn to the surface of the low gradient channel and rolled to the mouth of the high gradient channel where they are siphoned in and captured on the internal wire. This design allows very high throughput while maintaining a very small capture volume.

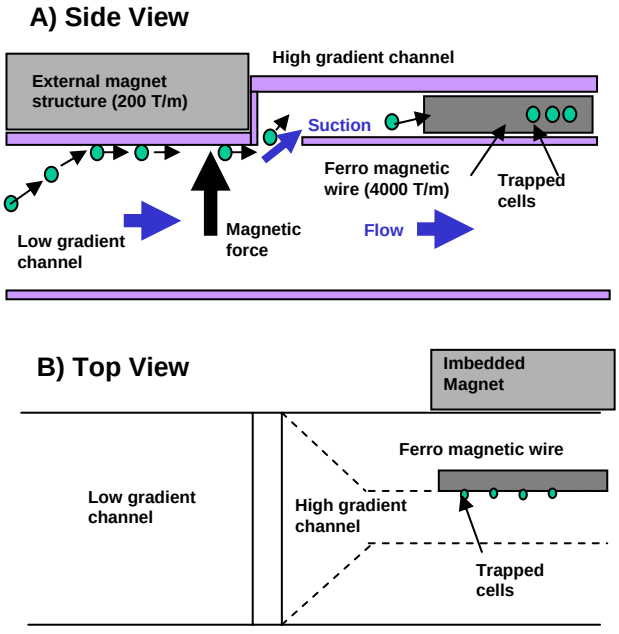

Fig. 1 Side and top schematic of the integrated high and low gradient channels. The external magnet structure consists of two neodymium magnets laid sided by side with

opposite poles facing the channel. The imbedded magnet magnetizes the wire in the plane of the channel width.

2.3 Device modeling

Two 2-dimensional single particle trajectory models based on magnetic and hydrodynamic force equations were developed to predict the efficiency of separation of magnetically labeled cells traveling in pressure driven flow. The first model tracks randomly distributed cells in a channel exposed to a constant externally generated magnetic gradient perpendicular to flow (low gradient channel). The equation governing the position of a cell in this model is [6]:

$$x = Q\,[3b^2(z_0-z) + z^3-z_0^3]\,/4u_z b^3 w$$

where x is position along the length of the channel, Q is the volumetric flow rate, **b** is the half height of the channel, z_0 is the initial height position of the center of the cell (relative to the channel center, z is the final position and u_z is the capture velocity in the height direction. This velocity is the magnetically induced velocity plus the sedimentation velocity. Note that the sedimentation velocity becomes negative when the system is inverted as in figure 1.

The second model tracks randomly distributed cells in a channel exposed to the variable gradient magnetic field created by a single integrated ferromagnetic wire(high gradient channel). The equation governing the position of a cell in this model are [8]:

For the r axis along the radial axis of the wire

$$r = \frac{1}{4}\sqrt{-\frac{50\cos(2\theta)}{\pi} + 16\,C\,|\sin(2\theta)|}$$

and for the z axis along the axis of flow

$$z = \frac{V_0\left(\frac{1}{2}K^2\ln\left(\frac{\tan(\theta_i)}{\tan(\theta)}\right) - K(r_i^2 - r^2) - \frac{1}{2}(K^2+C^2)(\cos(2\theta_i) - \cos(2\theta))\right)}{V_m}$$

where

$$K := \frac{M_s}{2\mu H_0} \qquad , \qquad V_m := \frac{2\chi M_s H_0 R^2}{9\eta a}$$

and where C is a constant determined by initial conditions M_s is the magnetization saturation of the wire, μ is the magnetic permeability of free space, H_0 is the magnetizing field R is the cell radius, χ is the magnetic susceptibility of the cell η is the viscosity of the medium and a is the radius of the wire. For a full treatment see Birss et. al. [8] Note that magnetic velocity is not constant and the directly measured cell velocities cannot be used. Instead magnetic susceptibility χ is calculated for the equivalent magnetizing field from the magnetic velocity.

Cell trajectories were calculated for random initial positions using the above equations in Maple 9 spreadsheets. The percentage of initial cell trajectories reaching the respective low and high gradient capture surfaces was determined for each flow rate tested experimentally.

3 RESULTS

The experiments designed to test the trajectory models agree fairly well with theory. This fit is improved in most all cases by adding a simple modification to account for lift forces generated at higher flow rates by excluding a small subset of the random initial target cell positions near the channel walls.

3.1 Low gradient channel in buffer

Figure 2 below shows the experimental capture data (points) and models (lines) for the low gradient channel at the higher flow rates tested. Magnetic gradients of 150 T/m and 55 T/m are shown as well as the 150 T/m gradient with the channel inverted and gravity acting against the magnetic force. While this configuration reduces overall capture rate it improves purity by allowing unlabeled cells to settle away from the capture surface. Also tested but not shown were gradients 55T/m in inverted configuration, 33T/m both upright and inverted and sedimentation with no magnetic field. 55T/m and 150 T/m in 50% mouse blood were also tested. See section 3.3

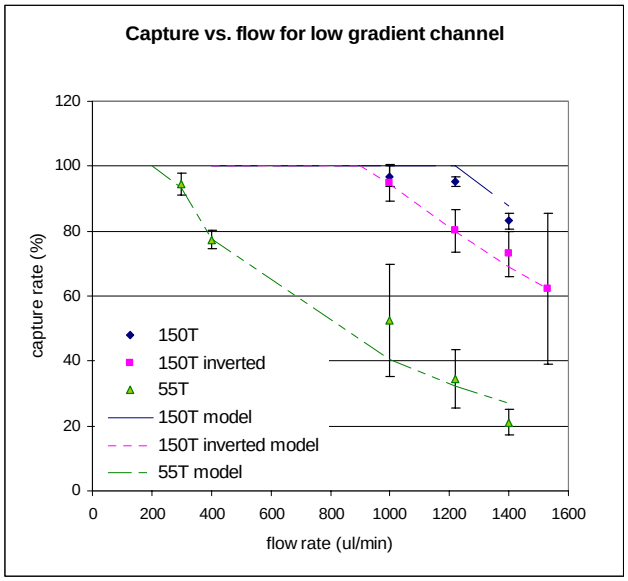

Fig. 2 Experimental data and corresponding capture models for the low gradient channel.

Table 1 shows the capture velocities for the populations tested. Sedimentation velocities for a typical cell are only around 2 μm/s. Magnetic velocities for real cells in a 150

T/m gradient with a 0.7 T field range from about 10 μm/s for a weakly labeled cell to > 100 μm/s for strongly labeled cells.

Table1
Capture velocities for various magnetic fields in μm/s

Grav -ity	*33.5T/m + g*	*55T/m + g*	*150T/m +g*	*55T/m -g*	*150T -g*
7.01	20.0	31.1	88.9	17.1	74.9

3.2 High gradient channel in buffer

Figure 4 shows the experimental results and models for the high gradient channel.

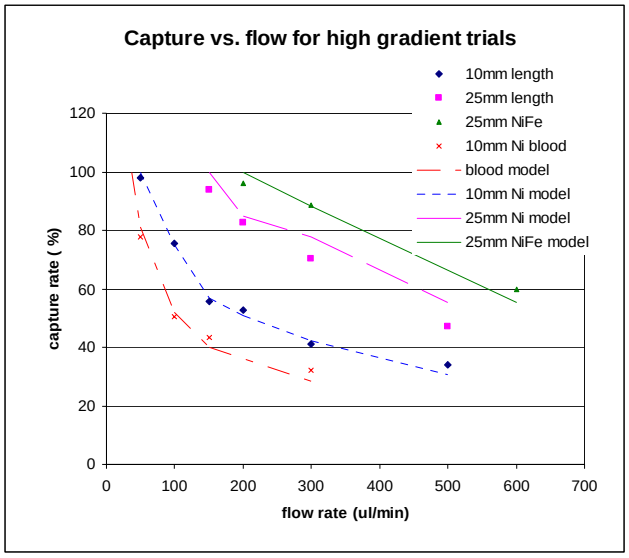

Figure 4. Capture vs. flow rate for the high gradient channel experiments and models.

The external field for these experiments was ~ 0.25 T. This corresponds to a calculated magnetic susceptibility for the model of ~ 1300.

3.3 Separations in blood

For both low and high gradient channels, the separation in 50% mouse blood showed a dramatic decrease in effective capture velocity. While each set of data could be fit reasonably well by reducing the effective magnetic velocity (or magnetic susceptibility in the high gradient case) by a single percentage, a trend of lower effective velocity reduction could be seen with increasing flow rate. This trend might be explained by shear dependent reduction of the viscoelasticity of blood but more experiments must be done to clearly define this relationship. The curve for blood in figure 4 (high gradient) used a 42% reduction in magnetic susceptibility and a similar fit for the low gradient channel shows a 48% reduction in magnetic velocity.

4 CONCLUSION

The primary goal of this research was the development of theory, methods and prototypes for solving the problem of high efficiency capture of rare target cells from clinical blood samples in microchannels. These tools could result in more efficient and specific isolation of disseminated tumor cells for diagnoses in cancer patients. They could also improve assay accuracy and reduce cost and assay time by allowing for easier integration of automated, operator error free diagnostic systems.

The results of this research show that model cells with similar magnetic moments to clinical targets labeled with colloidal immunomagnatic labels can be efficiently separated and captured at flow rates that would allow processing of milliliter samples in just a few minutes. Futhermore this separation and capture can be accomplished in nanoliter volumes.

REFERENCES

[1] Edelstein, R.L., et al., The BARC. Biosensors and Bioelectronics, 2000. **14**: p. 805-813.

[2]Terstappen, L.W.M.M. and P.A. Liberti, Methods for biological substance analysis employing internal magnetic gradients separation and an externally applied transport force. 2000, Immunivest Corporation: USA15-4215, 1959.

[3] Vlems, F., et al., Detection and Clinical Relevance of Tumor Cells in Blood and Bone Marrow of Patients with Colorectal Cancer. Anticancer Research, 2003. **23**: p. 523-530

[4] Vlems, F., et al., Reliability of quantitative reverse-transcriptase-PCR-based detection of tumor cells in blood between different laboratories using a standardised protocol. European Journal of Cancer, 2003. **39**: p. 388-396.

[5] McCloskey, K.E., J.J. Chalmers, and M. Zborowski, *Magnetophoretic Mobilities Correlate to Antibody Binding Capacities.* Cytometry, 2000. **40**: p. 307-315.

[7] Munn, L.L., R.J. Melder, and R.K. Jain, *Analysis of Cell Flux in the Paralell Plate Flow Chamber: Implications for Cell Capture Studies.* Biophysical Journal, 1994. **67**: p. 889-895.

[8] Birss, R.R., R. Gerber, and M.R. Parker, *Theory and Design of Axially Ordered Filters for High Intensity Magnetic Separation.* IEEE Transactions on Magnetics, 1976. **MAG-12**(6): p. 892-900.